Flexible Multimode Polymer Waveguide Arrays for Versatile High-Speed Short-Reach Communication Links

Fengyuan Shi, Nikolaos Bamiedakis, Peter P. Vasil'ev, Richard V. Penty, *Senior Member, IEEE*, Ian H. White, *Fellow, IEEE*, and Daping Chu, *Senior Member, IEEE*

***Abstract*—Optical interconnects play an important role in enabling high-speed short-reach communication links within next-generation high-performance electronic systems. Multimode polymer waveguides in particular allow the formation of high-capacity optical backplanes and cost-effective board-level optical interconnects. Their formation on flexible substrates offers significant practical advantages and enables their deployment in environments where shape and weight conformity become particularly important, such as in cars and aircraft. However, bending and twisting of flexible multimode waveguides can have a significant effect on their optical transmission performance due to mode loss and mode coupling. Moreover, the magnitude of the induced effects strongly depends on the launch conditions employed. In this paper, therefore, we present detailed loss, crosstalk, and bandwidth studies on flexible multimode waveguide arrays for different launch conditions regarding their use in real-world systems. The minimum radius to achieve a 1 dB excess bending loss is obtained for each launch condition as well as the crosstalk degradation due to bending. It is shown that for a 50 μm MMF input, a 6 mm bending radius is required for excess losses below 1 dB, while crosstalk below -35 dB is obtained in adjacent waveguides even under strong bending. Moreover, it is found that twisting has a small effect on the loss and crosstalk performance of the samples. Excess twisting loss less than 0.1 dB and crosstalk of -40 dB are obtained for three full 360° turns under a 50 μm MMF launch. Finally, the bandwidth studies carried out on the samples indicate than no significant bandwidth degradation is induced due to sample bending, with bandwidth-length product values larger than 150 GHz $\times$ m obtained for restricted launches. The set of results presented herein specify the deployment of this flexible polymer multimode waveguide technology in real-world systems and demonstrate its strong potential to implement low-loss high-bandwidth optical interconnects.**

***Index Terms*—Bandwidth studies, flexible interconnects, multimode waveguides, optical interconnections, polymer waveguides, printed flexible waveguides.**

Manuscript received November 8, 2017; revised February 2, 2018; accepted March 8, 2018. Date of publication March 20, 2018; date of current version May 15, 2018. This work was supported by the Jaguar Land Rover through the CAPE LEASA Project. *(Corresponding author: Daping Chu.)*

F. Shi, N. Bamiedakis, R. V. Penty, I. H. White, and D. Chu are with the Electrical Engineering Division, Department of Engineering, University of Cambridge, Cambridge CB3 0FA, U.K. (e-mail: fs431@cam.ac.uk; nb301@cam.ac.uk; rvp11@cam.ac.uk; ihw3@cam.ac.uk; dpc31@cam.ac.uk).

P. P. Vasil'ev is with the Electrical Engineering Division, Department of Engineering, University of Cambridge, Cambridge CB3 0FA, U.K., and also with the PN Lebedev Physical Institute, Moscow 119991, Russia (e-mail: pv261@cam.ac.uk).

Color versions of one or more of the figures in this paper are available online at http://ieeexplore.ieee.org

Digital Object Identifier 10.1109/JLT.2018.2816562

I. Introduction

OPTICAL interconnects have attracted great interest for use in short-reach high-speed communication links in recent years as they offer significant advantages over traditional copper links. They exhibit large bandwidth, reduced power consumption and immunity to electromagnetic interference (EMI) [1], [2]. Various technologies are being developed for use at the different interconnection levels: board-to-board, chip-to-chip and on-chip. Technological approaches to date have included using free-space [3], [4], fibre-based [5], [6], III-V and Si photonics [7], [8] and polymer-based interconnects [9], [10]. In particular, multimode polymer waveguides are promising for use in board-level optical interconnections as such waveguides exhibit excellent optical properties [11] and can be cost-effectively and directly integrated on standard printed circuit boards (PCBs). Significant research has been carried out in recent years by academia and industry resulting in detailed waveguide studies [12]–[14] and numerous demonstrations of optical backplanes based on polymer multimode waveguides [15]–[18]. Moreover, these waveguides have been shown to exhibit relatively large bandwidth-length products in excess of 30 GHz $\times$ m [19] despite their highly multimode nature, whilst data transmission of 40 Gb/s using non-return-to-zero (NRZ) modulation [20] and 56 Gb/s using 4-level pulse-amplitude modulation (PAM-4) [21] have been demonstrated over a 1 m long spiral multimode polymer waveguide. The combination of large parallel waveguide arrays and high-speed VCSEL arrays can provide low-cost optical board-level interconnection with aggregate data capacities over 1 Tb/s [22].

The formation of polymer waveguides on flexible substrates offers shape flexibility, lightweight and reduced thickness optical interconnects for chip-to-chip links, but can also enable a wider range of applications where shape conformity and weight restrictions become particularly important, such as in automotive and aircraft environments [23]. Optical links are currently deployed in in-car networks mainly using plastic optical fibres (POFs) and optical data bus systems, such as in Media Oriented Systems Transport (MOST) [24] and Intelligent Transportation Data Bus (IDB) systems [25]. Next-generation cars and aircrafts have requirements for enhanced passenger experience, and the advent of autonomous vehicles, whose successful operation rely on numerous sensors and cameras, require short-reach

high-speed data communication links. Flexible polymer waveguides can offer a very large bandwidth and, at the meantime, exhibit lower weight and can be bent with a smaller radius than POF. As a result, they can be used to form cost-effective high-speed optical buses for the above applications.

Various flexible multimode polymer waveguide technologies have been developed in recent years by different groups and some studies on the performance of the waveguides under flexure have been reported [26]–[32]. For example, in [28], bending loss measurements on flexible multimode waveguides using a 62.5 μm multimode fibre (MMF) input indicate that no significant bending loss is induced for a 360° bend for a radius larger than 3 cm. In [30] bending loss studies are carried out on flexible waveguides, demonstrating a 4.3 dB excess loss when the sample is bent at 5 mm under a 9 μm SMF input. Similar studies have been reported in [26]. The focus however of these publications has been the development of the flexible waveguides and the related opto-electronic sub-assemblies rather than the performance of the waveguides when the flexure is applied. Additionally, none of the aforementioned studies considers the fact that loss performance of such waveguides strongly depends on the launch conditions employed due to their highly-multimoded nature. In this work therefore, we present detailed studies on the effects of bending and twisting on the loss, crosstalk and bandwidth performance at 850 nm of $\sim 50 \times 50\,\mu\text{m}^2$ polymer multimode waveguide arrays on flexible substrates. The performance of the flexible waveguides is investigated under different launch conditions, ranging from restricted to relatively overfilled, providing useful guidelines for their successful deployment in real-world systems. The minimum radius of curvature to achieve excess bending losses below 1 dB and the crosstalk in adjacent waveguides are obtained for the different launch conditions. For a 50 μm MMF input, the 1 dB excess loss radius is found to be 6 mm, while crosstalk values below -35 dB are obtained. Similar studies are performed when the flexible waveguides are twisted and it is shown that this type of deformation has only a small effect on their loss and crosstalk performance as long as the sample width is kept small enough. For example, 4 full 360° twists result in an excess loss below 0.8 dB even for a relatively overfilled 100 μm MMF input and no significant degradation in crosstalk performance when compared with straight waveguide samples. Moreover, the bandwidth measurements reveal a bandwidth-length product in excess of 100 GHz $\times$ m under a restricted launch, and no significant bandwidth degradation when bent down to 3 mm of radius. The set of results presented herein indicate robust optical properties of flexible polymer waveguides under different flexure environments, which demonstrates its strong potential to implement low-loss high-bandwidth optical interconnects.

The rest of the paper is organised as follows. Section II introduces the flexible waveguide technology used in this work, while Sections III and IV present the loss and crosstalk performance of the flexible waveguide samples under flexure (bending and twisting, respectively). Section V describes the bandwidth measurements on the samples, while Section VI discusses some of the points related to the measurements and obtained results. Finally, Section VII presents the conclusions.

Fig. 1. Images of two samples used in these studies, 13.5 (lower) and 24 cm (upper) in length.

II. Flexible Multimode Polymer Waveguides

The polymer waveguides employed in this work are fabricated from siloxane materials developed by Dow Corning Corporation for use in PCB board level integration and optical backplanes for server racks in data centers. These materials (core: WG-1020 and cladding: WG-1023) can be deposited on various substrates, exhibit very low loss ($\sim$0.04 dB/cm) at the datacommunication wavelength of 850 nm, can withstand the high temperatures (in excess of 350 °C) associated with solder reflow and board lamination, and long-term stability [28]. The waveguides used in this work are fabricated on 125 μm thick polyimide substrates using conventional photolithography. They have a cross section of $\sim 50 \times 50\,\mu\text{m}^2$ as this is comparable to the core diameter of standard 50 MMF and offer a 1 dB alignment tolerance of ± 10 μm that can be readily achieved with conventional pick-and-place tools [11]. The refractive index difference between the core and cladding materials is $\sim$0.02 at 850 nm, yielding a numerical aperture (NA) of $\sim$0.25 for the waveguides. Samples of different lengths (13.5 and 24 cm) are produced. The waveguide facets are exposed with a dicing saw and no polishing steps are undertaken to improve the quality of the facets produced. Fig. 1 shows an image of the two different samples.

Each flexible sample contains an array of 12 waveguides with a pitch of 250 μm. This matches the standard pitch of multimode fibre ribbons and VCSEL arrays. The samples can be bent down to 1 mm radius without any cracking or delamination.

III. Bending Loss Performance

A. Experimental Setup and Launch Conditions

Due to the highly multimode nature of these waveguides, the bending loss performance of the flexible polymer waveguides is investigated under different launch conditions. In this work three different input launch conditions ranging from restricted to relatively overfilled are employed: a 4/125 μm SMF (NA of 0.13), a graded index 50/125 μm MMF (NA of 0.2) and a 100/140 μm MMF (NA of 0.29) input with a mode mixer (MM, Newport FM-1). The 4/125 μm SMF input excites the lowest number of modes inside the polymer waveguide, while the 100/140 μm MMF input with a mode mixer excites the largest. This launch represents a 'worst-case' excitation with respect to bending loss as a larger percentage of the power is coupled to the higher order modes, which are more susceptible to bending loss at the waveguide input. The 50/125 μm MMF input consists of a launch that is between these two extremes and represents a common multimode fibre. Near-field images of the cleaved end of the input fibre for the 3 launches are recorded while the far-field profile of the emitted beam is also measured (Fig. 2).

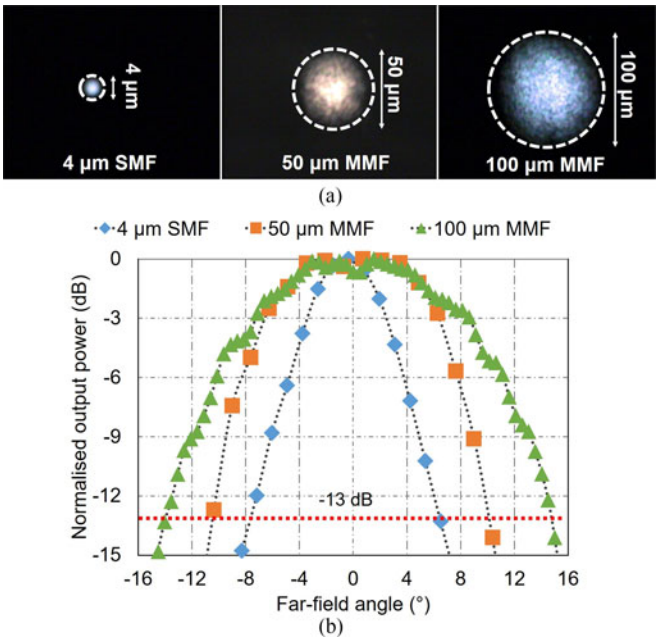

Fig. 2. (a) Near-field image of the cleaved end of the input fibre and (b) far-field intensity profile for the 3 launches studied. The −13 dB points correspond to the 5% far-field intensity.

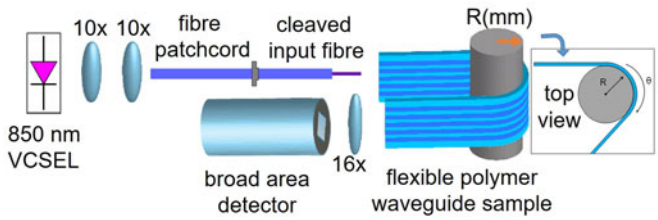

Fig. 3. Experimental setup for bending loss studies.

The 5% far-field intensity angle (FFA) of each input is found from the measured normalised far-field profile (−13 dB points) and is used to characterise the launch condition by comparing it with the waveguides acceptance angle ($\mathrm{AA}_{wg} \sim 14.5°$). The 5% half FFA of the 3 input fibres used in the experiments is found to be 7.1°, 10.9° and 16° for the SMF, 50 μm MMF and 100 μm MMF input respectively, while the respective calculated values using the fibre NA are 7.5°, 11.5° and 16.8° for the SMF, 50 μm MMF and 100 μm MMF input respectively. The measured FFA values are in good agreement with the theoretical values and confirm the characterisation of the SMF input as restricted launch ($\mathrm{FFA} < \mathrm{AA}_{wg}$), the 50 μm MMF as typical ($\mathrm{FFA} \sim \mathrm{AA}_{wg}$) and the 100 μm MMF input as relatively overfilled ($\mathrm{FFA} > \mathrm{AA}_{\mathrm{wg}}$).

The experimental setup used in the bending loss measurements is shown in Fig. 3, while an image of a bent waveguide sample is shown in Fig. 4.

An 850 nm vertical-cavity surface-emitting laser (VCSEL) is used as the light source and the emitted light is coupled into fibre patchcord via a pair of 10× (NA of 0.25) microscope objectives. A second fibre patchcord of the same type with a cleaved end is used to couple the light into the waveguides. The

Fig. 4. Images of the bent waveguide sample (a) under room lighting and (b) illuminated with red light.

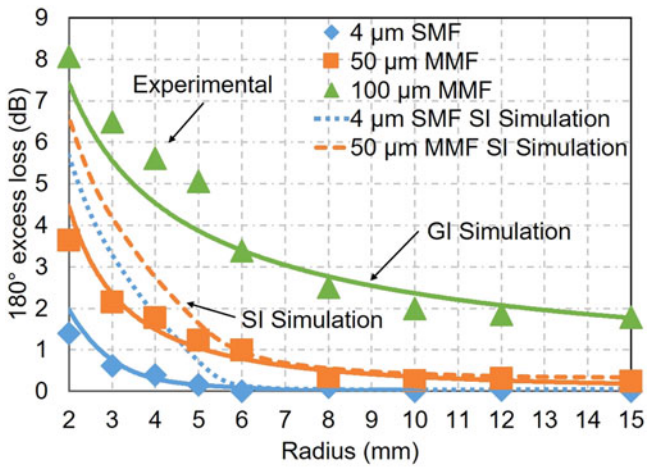

Fig. 5. Excess bending loss for different bending radii, experimental (symbols) and simulation (lines) results.

flexible waveguide sample is bent around a cylindrical mandrel for a given angle of curvature, while a 16× microscope objective (NA of 0.32) is used to collect the transmitted light at the waveguide output and focus it onto an optical powermeter. The NA of the employed output lens is larger than that of the waveguides (∼0.25), ensuring therefore that all transmitted light is collected at the waveguide output. Index matching gel is applied at the waveguide input to minimise Fresnel loss and scattering loss due to surface roughness. Mandrels of different radius of curvature between 2 and 15 mm are employed for the measurements, while the bending angle is varied between 0° and 180°. For these measurements, the 13.5-cm long sample is employed. For each measurement and launch condition studied, the insertion loss of all 12 waveguides on the sample is obtained and the average value is calculated. In order to obtain the excess loss due to waveguide bending, the insertion loss of waveguides when no flexure is applied (straight waveguides) is also measured for the different launch conditions. The average insertion loss for the straight waveguides is found to be ∼1.4, 1.5 and 5.9 dB for the 4 μm SMF, 50 μm MMF and 100 μm MMF launches respectively.

B. Bending Loss Versus Radius of Curvature

Fig. 5 shows the average excess bending loss as a function of radius of curvature for a 180° bend. As expected, the use of the 100 μm MMF input results in large excess bending loss due

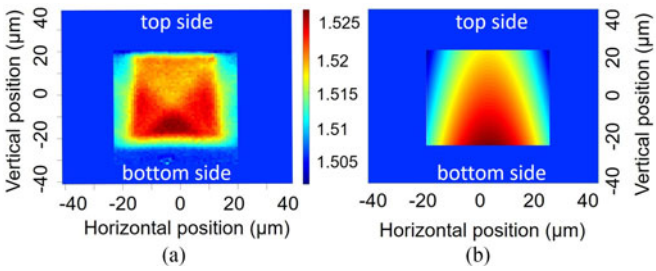

Fig. 6. (a) Measured refractive index profile of the waveguide sample on rigid substrate and (b) simulated profile for flexible waveguide studies.

to the excitation of higher order modes at the waveguide input. For the less overfilled launches however, a good bending loss performance is recorded. The minimum radius to achieve 1 dB bending loss is found to be 3 and 6 mm for the SMF and 50 μm MMF inputs respectively.

Ray tracing simulations are carried out with ZEMAX to validate the observed results. The refractive index (RI) profile of the waveguide is assumed to have a gradient profile that is similar to the profile obtained from waveguide samples fabricated on rigid substrates as shown in Fig. 6 [33]. The different launch conditions used in the experiments are implemented in the simulations by matching the angular profile of the ray source at the waveguide input to the far-field profile of the respective fibre input (Fig. 2). The excess bending loss is once more obtained by subtracting the insertion loss of the waveguides when no flexure is applied (straight waveguides). The obtained simulation results are plotted in Fig. 5 with solid lines. Good agreement is achieved between the simulated and experimental curves.

Simulations are done to assess the effect of the graded-index (GI) shape in the RI profile on the loss performance of these flexible waveguides in comparison with the case of the step-index (SI) shape. It is assumed that the waveguides have the same RI difference between the core and cladding and the same dimensions but with a uniform RI profile over its cross section. The obtained results are also plotted in Fig. 5 for a SMF and a 50 μm MMF input. As expected, the graded-index profile provides an improved bending loss performance due to the increase mode confinement within the waveguide core.

C. Bending Direction

Due to the asymmetry in the RI profile of the waveguides, the bending loss is expected to be different when the same sample is bent in two opposite out-of-plane directions as shown Fig. 7(a): upwards (with the top side located in the inside part of the bend) and downwards (bottom side located in the inside part of the bend). Measurements are carried out to quantify this effect on a 24 cm-long sample when the sample is bent in these two directions using the setup shown in Fig. 3. It is expected that the upward bending (type A) should result in a larger excess loss as the region of higher RI is positioned towards the outer side of the bend, resulting in a worse mode confinement, while the difference in performance is expected to be much larger for tighter bends (smaller radii) and more overfilled inputs. Fig. 7(a)

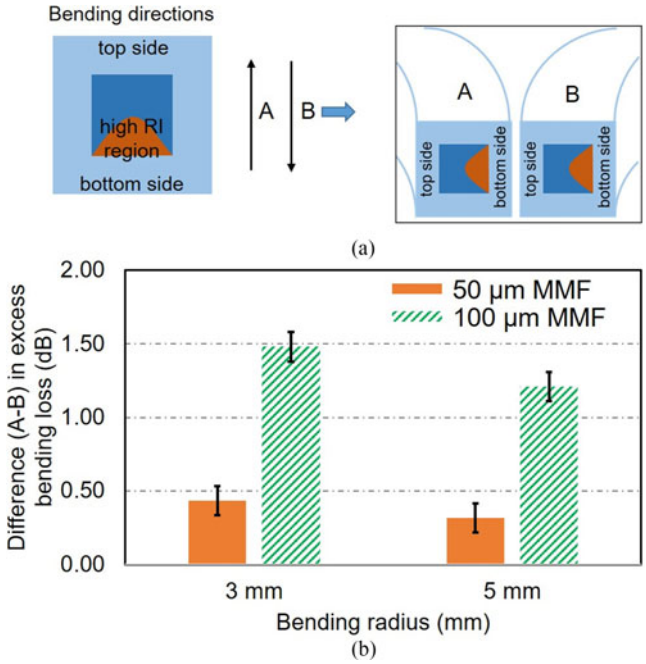

Fig. 7. (a) Schematic illustration of the two out-of-plane bending directions and (b) difference in excess bending loss between directions A and B when the sample is bent 180° with a 3 and 5 mm radius, respectively.

shows the difference in obtained excess bending loss between the upward (type A) and downward (type B) bends for 3 and 5 mm radius.

The obtained results are in agreement with the expected performance. The 100 μm MMF input results in a 1.5 dB difference in loss between the two bending directions for the smaller 3 mm radius, whilst the 50 μm MMF input yields a much smaller difference of $\sim$0.4 dB for the same bending radius. Overall, the obtained results indicate a small difference in bending losses between the two opposite bending directions.

D. Bending Loss vs Angle of Curvature

The bending loss of the waveguides is also recorded when the angle of curvature is varied between 0° and 180° for a fixed radius of curvature. Fig. 8 shows the obtained excess loss for 3 and 5 mm radius for the different launch conditions.

It can be observed that the excess bending loss curve exhibits a decreasing gradient with increasing bending angle. Similar behaviour has been observed in multimode waveguide crossings [34] and it can be explained by the fact that the majority of the power in the higher order modes is lost in the initial parts of the bends, with the remaining lower order modes, that exhibit lower bending loss, left to propagate along the remaining length. The effect is more pronounced for the 100 μm MMF input as a higher percentage of power is coupled to the higher order modes which are more susceptible to bending loss.

Near-field images of the waveguide output are recorded for the different angles of curvature when a 3 mm radius is used (Fig. 9). The images confirm the above observations, clearly showing the suppression of the higher order modes for the

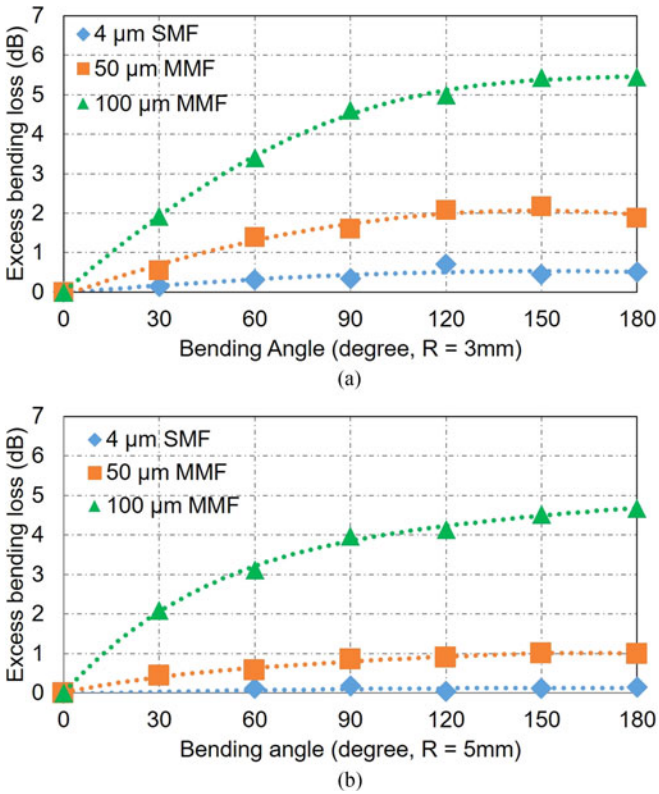

Fig. 8. Excess bending loss as a function of bending angle for (a) 3 mm and (b) 5 mm radius for the three launch conditions studied.

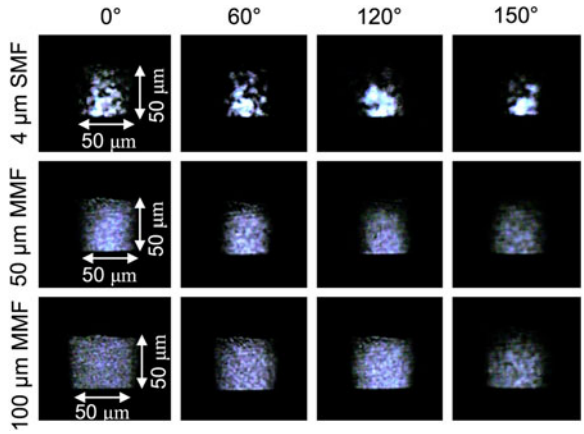

Fig. 9. Near-field images of the waveguide output for different bending angles for a 3-mm radius.

100 μm launch as the bending angle increases. Alternatively, for the SMF input, the light is well confined at the waveguide bottom centre (region of higher RI, Fig. 6) with the relative intensity over the waveguide core not significantly changing.

E. Crosstalk Performance

The crosstalk performance of the 24-cm long sample under flexure (180° bend) is also investigated. The measurement setup employed is similar to that used in the bending loss

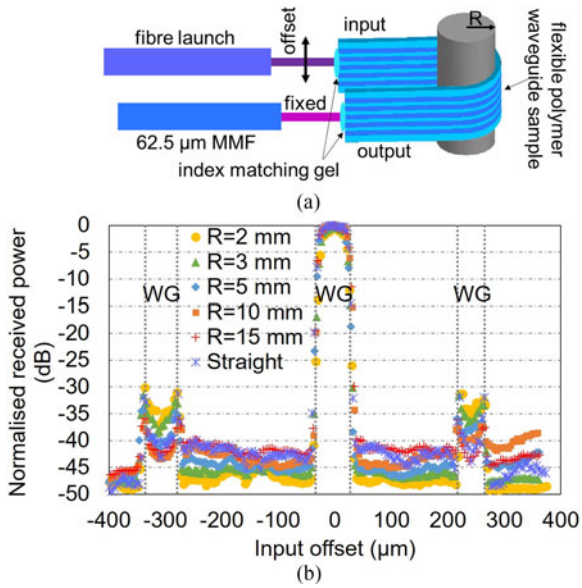

Fig. 10. (a) Schematic of crosstalk measurement of bent waveguide sample and (b) normalised received power at the waveguide output as a function of the input position for different bending radii for the 4 μm SMF input.

measurements (Fig. 3), but for the lens at the waveguide output which is replaced by a 62.5/125 μm graded index MMF [Fig. 10(a)]. The use of the fibre is preferred for these measurements as it minimises the collection of stray background light at the waveguide output, while the size and NA of the employed 62.5 μm MMF ensure the collection of the majority of the power received at the waveguide output. The output fibre is aligned with one of the waveguides, while the position of the input fibre is offset between the two adjacent waveguides. The optical power received for each input position is recorded and the crosstalk is derived by comparing the output recorded when the input is well aligned with each of the adjacent waveguides. The measurement is repeated for the different launch conditions and for different bending radii. For these measurements, index matching gel is applied at both the input and output waveguide facets to minimise additional loss and crosstalk due to facet roughness. Fig. 10(b) shows the normalised received power at the waveguide output as a function of the position of the input fibre for the 4 μm SMF launch for different bending radii. The small peaks observed in the figure occur when the SMF input is positioned at the waveguide edges (left/right sidewall) and is due to the additional scattering induced by the core-cladding boundary. This effect is observed in all measurements (straight and bent waveguides), but becomes less pronounced as larger and more overfilled inputs are employed.

Fig. 11 summarises the obtained crosstalk values as a function of bending radius for the different launch conditions studied. The crosstalk is found to increase slightly with decreasing bending radius with worst-case values of -36, -30 and -26 dB recorded for the SMF, 50 μm MMF and 100 μm MMF input respectively for the 2 mm bend. In all cases, the obtained crosstalk values are below -25 dB, indicating good performance even under tight bends and relatively overfilled launches.

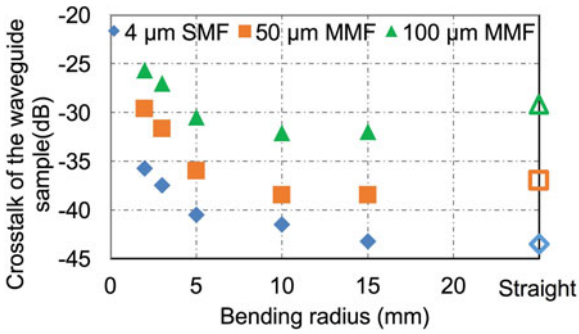

Fig. 11. Crosstalk performance of the flexible waveguide sample when bending at different radii under different launch conditions.

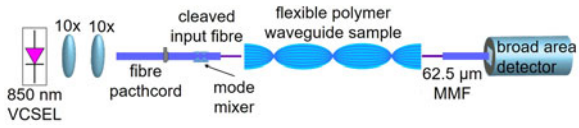

Fig. 12. System setup for the twisting loss experiment.

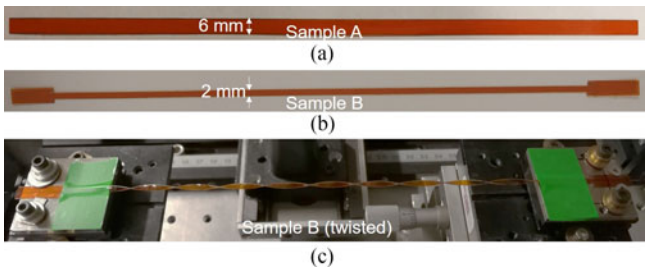

Fig. 13. Flexible polymer waveguide samples used in twisting loss measurements: (a) sample A with 6 mm width and (b) sample B with 2 mm width, and (c) image of twisted sample B under 5 full (360°) twist turns.

IV. Twisting Loss and Crosstalk Performance

A. Twisting Loss

The loss performance of the flexible sample is also investigated under in-plane twist using the same launch conditions (Fig. 12).

For this measurement, the longer waveguide sample, 24 cm in length, is used as it allows larger number of full twist turns to be applied. The average insertion loss of the waveguides is measured when no twist is applied and this is found to be ~3.2, 3.6 and 9 dB for the 4 μm SMF, 50 μm MMF and 100 μm MMF inputs respectively. In order to apply the twist, one side of the sample is clamped while the other side is rotated along the waveguide axis an integer number of 360° turns (Fig. 13). The waveguide sample is stretched in order to ensure that the length of the twisted sample is similar to that when no twist is applied (straight sample), and is then clamped. The insertion loss of the waveguides is subsequently measured. Fig. 14 shows the obtained average twisting excess loss as a function of the number of full 360° twists for the different launch conditions for the sample A (unfilled bars).

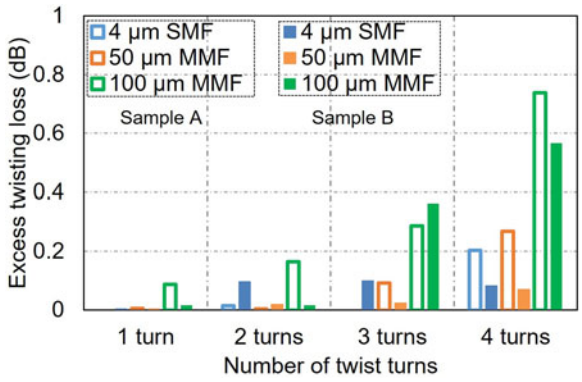

Fig. 14. Average twisting excess loss for samples A and B as a function of the number of full 360° twists for the different launch conditions.

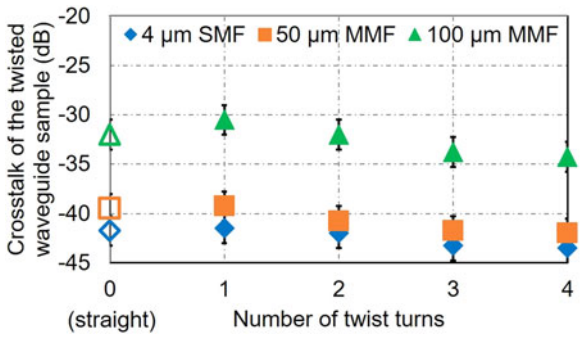

Fig. 15. Crosstalk of a twisted flexible waveguide sample for different numbers of full twisting turns and the different launch conditions (fibre diameters).

In order to minimise the effect of lateral tension on the sample due to the twist, the sample width is reduced from 6 to 2 mm [Fig. 13(a) and (b)] and the twisting loss is measured once more. For the sample with reduced width (sample B), only 4 waveguides are operational and these are used to determine the average insertion loss for each number of turns. The obtained excess loss is shown in Fig. 14 with filled bars.

For all launch conditions and for both samples, the excess twisting loss is below 0.8 dB even for 4 full 360° turns. For the SMF and 50 μm MMF input, the excess twisting loss for up to 4 full turns for sample A is below 0.3 dB. The reduction of the sample width in sample B minimises the lateral tension induced on the sample, resulting therefore in an improved twisting loss performance for all launches. Negligible excess loss of 0.1 dB is obtained for sample B for the SMF and 50 μm MMF inputs for up to 4 full twists turns.

B. Crosstalk Performance

The crosstalk performance of the samples is also investigated using the same experimental setup. Fig. 15 shows the obtained crosstalk values of the twisted waveguide sample as a function of the number of full twisting turns for the different launch conditions studied. No significant difference in crosstalk performance is observed due to the waveguide twist with recorded

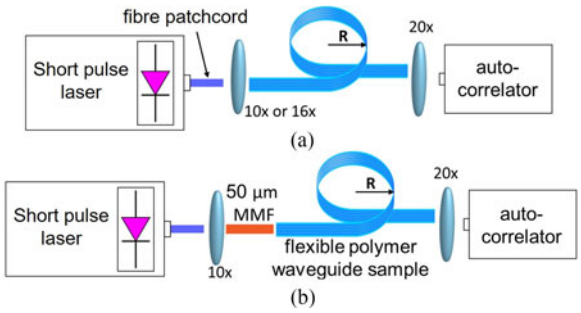

Fig. 16. Experimental setup for bandwidth studies using (a) a lens launch and (b) a 50 μm MMF input.

crosstalk values ~ -40 dB for a well-aligned SMF and 50 μm MMF inputs and -30 dB for the 100 μm MMF input.

Overall, it is shown that twisting has a negligible effect on the loss and crosstalk performance of the flexible waveguide samples as long as care is taken to minimise any lateral tension in the sample induced by the twisting (i.e., reduced sample width). In the case however that this is not possible, the twisting loss performance depends on the twisting angle and applied force and the sample's geometric and mechanical characteristics (length, width, thickness and elasticity) [35]. Depending on these parameters, different forms of twisted ribbons can be generated (e.g., bulking, self-contact, helicoid) which have different strain and curvature profiles along the sample [36] and therefore, result in different twisting excess loss. A detailed study is underway to fully characterise these different types of deformations and correlate them with the twisting loss performance of flexible waveguide samples. The findings are expected to provide more specific design guidelines with respect to twisting loss performance.

V. Bandwidth Studies of Flexible Polymer Waveguide

The bandwidth of the flexible polymer waveguides is investigated when a flexure is applied. The waveguide bandwidth is estimated using pulse broadening measurements and is used to calculate the bandwidth-length product (BLP), a common metric used in multimode fibre transmission systems to quantify the induced dispersion. As the main dispersion component in such systems is multimode dispersion [37], its magnitude scales linearly with link length resulting in a constant BLP value that characterises the fibre performance [38]. A similar approach is taken here for these multimode waveguides. As a result, their BLP values under flexure and under different launch conditions are obtained. They can be used to find out the bandwidth of a waveguide with a given length under similar launch conditions.

The system setup is shown in Fig. 16. A short optical pulse is launched into the waveguides, and the dispersion induced by the waveguide for different launch conditions and different radii of curvature is obtained by recording the autocorrelation trace of the output pulse. By comparing the input and output pulses, the frequency response, and therefore the 3 dB bandwidth of the waveguide can be obtained. Similar studies on waveguides on rigid substrates have been reported in [37]. The input short optical pulse ($\sim$ 290 fs full width at half maximum) is generated at 787 nm using an erbium-doped fibre laser operating a 1574 nm and a frequency doubling crystal (MSHG1550-0.5-1). Different launches are employed at the waveguide input implemented with microscope objectives with different magnification: 10$\times$ and 16$\times$ and a short 50 μm MMF patchcord. The flexible sample is wrapped 360° around a cylindrical mandrel of a certain radius of curvature, with the position of the bend being roughly at middle of the waveguide length. The output light is collected with a 20$\times$ microscope objective and delivered to a matching autocorrelator. The autocorrelation trace of the received optical pulse is recorded and used to estimate the pulse shape using standard curve fitting and common pulse shapes such as Gaussian, Sech² and Lorentzian. Typically, restricted launches result in Sech²-shaped output pulses as these types of launches mainly excite lower order modes inside the waveguide that exhibit small differences in their group velocities. On the other hand, more overfilled or offset launches result in output pulses that are better fitted by Lorentzian-shaped pulses due to the excitation of higher order modes at the waveguide input and the larger induced multimode dispersion. The frequency response of the waveguide can be extracted by taking the Fourier transform of input pulse (back-to-back) and fitted output pulse. As a result, the bandwidth-length product of the waveguide under different bending radius can be determined by finding the 3 dB bandwidth value. For these measurements, the 24 cm long samples are employed. The far-field profile of the output beam is also recorded for the different launch conditions in order to characterise the modal excitation inside the waveguides. Fig. 17(a) shows the average BLP value as a function of the radius of curvature for the different launches while Fig. 17(b) indicates the respective 5% far-field intensity angle (FFA). The 5% FFA angle corresponding to the waveguide NA is also noted in the plot for reference.

BLP values larger than 150 GHz $\times$ m are recorded for all the launch conditions studied and employed bending radii. As expected, the use of the 50 μm MMF input results in lower bandwidth values due to the excitation of higher-order modes at the waveguide input. The lens input yields substantially larger BLP values $>$250 GHz $\times$ m. No significant degradation in bandwidth performance is observed when the waveguides are flexed, with similar BLP values obtained for the straight and bent waveguides down to 3 mm radius. The far-field measurements confirm the bandwidth observations, as they show no significant change in modal volume at the waveguide output even when the waveguides are bent down to 3 mm radius.

It should be noted that all the results shown here correspond to launches that relatively underfill the modal volume of the waveguides. More overfilled launches have been tested with the same setup, but the accuracy of the bandwidth estimation is inadequate due to poor fitting of the autocorrelation traces with standard pulse shapes. As a result, these are not presented and are subject to further study. For overfilled launches however, flexing the waveguides is expected to have a beneficial effect with respect to waveguide bandwidth when compared with the same waveguide without any flexure (straight) under the same launch, as higher order modes are suppressed along the bend reducing therefore multimode dispersion. Similar behaviour has

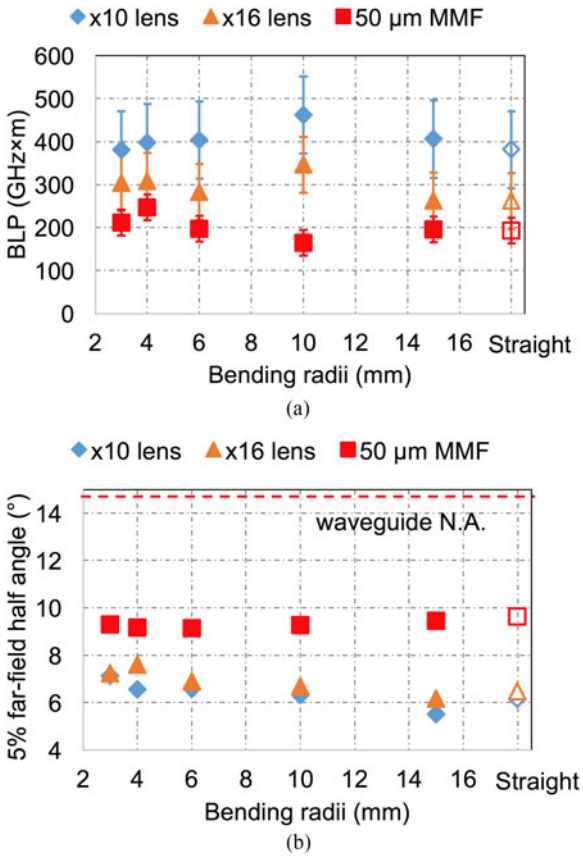

Fig. 17. (a) Bandwidth length product of the flexible polymer waveguide sample and (b) the 5% far-field half angle of the waveguide output laser beam.

been recorded in in-plane 90° bends and has been reported in [39].

VI. Discussion

A. Stress-Induced Effects

The magnitude of the applied tension on the samples in the bending and twisting experiments can have an important effect on their loss performance. As discussed in Section IV, the applied tension plays an important role in the twisting measurements as it affects the sample shape and the local radius of the curvature along its length and therefore its loss performance. In the case of an out-of-plane bending, high tension can result in stress-induced changes of the refractive index along the waveguide length as well as additional loss or mode coupling. In the measurements described here, care was taken not to apply high stress on the samples, and therefore we believe that any induced photo-elastic effects in our measured results should not be significant. Careful experimental work is required to quantify such induced effects, and we plan to study them in detail and report the outcome in a future publication.

B. Mode Mixing Due to Sample Bending

Mode mixing can have a significant impact on the performance of multimode waveguide systems. In general, mode mixing in multimode polymer waveguides has not been thoroughly studied and understood yet. Although our study over the years has hinted that the effect is not strong over the typical lengths of interest ($<$1 m) for board-level optical interconnects. For the flexible waveguides presented here, sample flexing could result in additional mode mixing in the waveguides and, in the case of restricted launches, result in significant bandwidth degradations. The bandwidth results obtained however, show no significant bandwidth change (and no significant change in far-field emission profile) when the samples are bent down to 3 mm radius. It therefore suggests that no significant additional mode mixing takes place in the waveguides due to the presence of the bend. The relative large (radius of $>$1 mm) and smooth bends used here are expected to have a much smaller effect than that of abrupt micro-bends (tight radius of $\sim$ μm) which are well-known to have a significant impact on the mode mixing in multimode fibres. Detailed studies are however required to provide quantitative information on the phenomena and we hope to be able to report further results in future publications.

C. Bend Insensitivity

The remarkable performance of the bending loss of these waveguides as observed here is mainly due to the large sizes in bending and their refractive index profiles. The relatively large RI difference between core and cladding of $\sim$0.02, the waveguide's large dimension and its graded-index RI profile provide a strong mode confinement (in comparison to that of single mode or few-mode waveguides) for the modes of lower orders which typically carry the majority of the optical power in such waveguides. The observed performance is similar or even slightly better than that obtained from a 90-degree in-plane waveguide bends fabricated with the same materials and similar waveguide dimensions (1 dB excess loss for a $\sim$8 mm radius under a 50 μm MMF input) [39]. The difference in performance can be attributed to the difference in the quality between the horizontal and vertical sidewalls of the waveguides. The vertical sidewalls typically exhibit a larger surface roughness than that of the horizontal (top and bottom) ones, resulting therefore in larger scattering losses when the waveguide modes are shifted towards the waveguide edges in the bend. Simulation studies on this effect are underway and we will report them in the near future.

VII. Conclusion

In this paper, the light transmission performance of flexible multimode polymer waveguide arrays is investigated in detail. The loss, crosstalk and bandwidth performance of flexible waveguide samples are studied when the samples are bent down to 2 mm of radius and twisted up to 4 full turns and when different launch conditions are employed at the waveguide input. The obtained results demonstrate very good performance and reliable operation even under tight bends and multiple twists. Bending down to 3 mm with relative low loss and small crosstalk degradation is achieved while it is shown that twisting has a negligible effect on the loss and crosstalk performance of the samples as long as lateral tension in the samples is minimised.

Finally, bandwidth studies reveal that, under restricted launches, no significant bandwidth degradation is observed due to sample bending. The set of results indicate robust optical performance of flexible multimode polymer waveguide arrays and demonstrate their strong potential for use in environments where shape flexibility and resistance to vibration and lateral movements are of great importance.

ACKNOWLEDGMENT

The authors would like to thank Dow Corning for the provision of the polymer waveguide samples through the CAPE OIC Future project.

REFERENCES

[1] D. Miller, "Device requirements for optical interconnects to silicon chips," *Proc. IEEE*, vol. 97, no. 7, pp. 1166–1185, Jul. 2009.
[2] H. Cho, P. Kapur, and K. C. Saraswat, "Power comparison between high-speed electrical and optical interconnects for interchip communication," *J. Lightw. Technol.*, vol. 22, no. 9, pp. 2021–2033, Sep. 2004.
[3] H. P. Kuo *et al.*, "Free-space optical links for board-to-board interconnects," *Appl. Phys. A*, vol. 95, pp. 955–965, Mar. 2009.
[4] K. Wang, A. Nirmalathas, C. Lim, E. Skafidas, and K. Alameh, "High-speed free-space based reconfigurable card-to-card optical interconnects with broadcast capability," *Opt. Express*, vol. 21, pp. 15395–15400, Jul. 2013.
[5] M. Schneider, T. Kühner, T. Alajoki, A. Tanskanen, and M. Karppinen, "Multi channel in-plane and out-of-plane couplers for optical printed circuit boards and optical backplanes," in *Proc. 59th Electron. Compon. Technol. Conf.*, 2009, pp. 1942–1947.
[6] R. Pitwon, A. Worrall, P. Stevens, A. Miller, K. Wang, and K. Schmidtke, "Demonstration of fully enabled data center subsystem with embedded optical interconnect," *Proc. SPIE*, vol. 8991, Mar. 2014, Art. no. 899110.
[7] G. Roelkens *et al.*, "III-V/silicon photonics for on-chip and intra-chip optical interconnects," *Laser Photon. Rev.*, vol. 4, pp. 751–779, 2010.
[8] M. Lipson, "Guiding, modulating, and emitting light on silicon-challenges and opportunities," *J. Lightw. Technol.*, vol. 23, no. 12, pp. 4222–4238, Dec. 2005.
[9] F. E. Doany *et al.*, "160 Gb/s bidirectional polymer-waveguide board-level optical interconnects using CMOS-based transceivers," *IEEE Trans. Adv. Packag.*, vol. 32, no. 2, pp. 345–359, May 2009.
[10] L. Schares *et al.*, "Terabus: Terabit/second-class card-level optical interconnect technologies," *IEEE J. Sel. Topics Quantum Electron.*, vol. 12, no. 5, pp. 1032–1044, Sep./Oct. 2006.
[11] N. Bamiedakis, J. Beals, R. V. Penty, I. H. White, J. V. DeGroot, and T. V. Clapp, "Cost-effective multimode polymer waveguides for high-speed on-board optical interconnects," *IEEE J. Quantum Electron.*, vol. 45, no. 4, pp. 415–424, Apr. 2009.
[12] A. Horimoto, K. Kitazoe, and R. Kinoshita, "Simple channel reconnection using polynorbornene based GI waveguide for optical interconnect," in *Proc. IEEE CPMT Symp. Jpn.*, Kyoto, Japan, 2015, pp. 122–125.
[13] R. Kinoshita, D. Suganuma, and T. Ishigure, "Accurate interchannel pitch control in graded-index circular-core polymer parallel optical waveguide using the Mosquito method," *Opt. Express*, vol. 22, no. 7, pp. 8426–8437, Apr. 2014.
[14] R. Dangel *et al.*, "Polymer-waveguide-based board-level optical interconnect technology for datacom applications," *IEEE Trans. Adv. Packag.*, vol. 31, no. 4, pp. 759–767, Nov. 2008.
[15] J. Beals *et al.*, "A terabit capacity passive polymer optical backplane based on a novel meshed waveguide architecture," *Appl. Phys. A, Mater. Sci. Process.*, vol. 95, pp. 983–988, 2009.
[16] N. Bamiedakis, A. Hashim, R. V. Penty, and I. H. White, "Regenerative polymeric bus architecture for board-level optical interconnects," *Opt. Express*, vol. 20, pp. 11625–11636, 2012.
[17] N. Bamiedakis, A. Hashim, R. V. Penty, and I. H. White, "A 40 Gb/s optical bus for optical backplane interconnections," *J. Lightw. Technol.*, vol. 32, no. 8, pp. 1526–1537, Apr. 2014.
[18] K. Schmidtke *et al.*, "960 Gb/s optical backplane ecosystem using embedded polymer waveguides and demonstration in a 12G SAS storage array," *J. Lightw. Technol.*, vol. 31, no. 24, pp. 3970–3975, Dec. 2013.
[19] N. Bamiedakis, J. Chen, R. V. Penty, and I. H. White, "Bandwidth studies on multimode polymer waveguides for >25 Gb/s optical interconnects," *IEEE Photon. Technol. Lett.*, vol. 26, no. 20, pp. 2004–2007, Sep. 2014.
[20] N. Bamiedakis *et al.*, "40 Gb/s data transmission over a 1-m-long multimode polymer spiral waveguide for board-level optical interconnects," *J. Lightw. Technol.*, vol. 33, no. 4, pp. 882–888, Feb. 2015.
[21] N. Bamiedakis *et al.*, "56 Gb/s PAM-4 data transmission over a 1 m long multimode polymer interconnect," in *Proc. Conf. Lasers Electro-Opt.*, San Jose, CA, USA, 2015, Paper STu4F.5.
[22] J. B. IV *et al.*, "Terabit capacity passive polymer optical backplane," in *Proc. Conf. Lasers Electro-Opt.*, San Jose, CA, USA, 2008, Paper CMG4.
[23] O. Strobel, R. Rejeb, and J. Lubkoll, "Optical polymer and polymer-clad silica fiber data buses for automotive applications," in *Proc. 7th Int. Symp. Commun. Syst. Netw. Digit. Signal Process.*, 2010, pp. 693–696.
[24] R. König and C. Thiel, "Media oriented systems transport (MOST®)-Standard für multimedia networking im fahrzeug/media oriented systems transport-standard for multimedia networking in vehicle environment," *It-Inf. Technol.*, vol. 41, pp. 36–43, 1999.
[25] Y. Dong and K. W. Martin, "Gigabit communications over plastic optical fiber," *IEEE Solid-State Circuits Mag.*, vol. 3, no. 1, pp. 60–69, Jan. 2011.
[26] R. Bruck *et al.*, "Flexible thin-film polymer waveguides fabricated in an industrial roll-to-roll process," *Appl. Opt.*, vol. 52, pp. 4510–4514, Jul. 1, 2013.
[27] G. Jiang, S. Baig, and M. R. Wang, "Flexible polymer waveguides with integrated mirrors fabricated by soft lithography for optical interconnection," *J. Lightw. Technol.*, vol. 31, no. 11, pp. 1835–1841, Jun. 2013.
[28] R. Dangel *et al.*, "Development of versatile polymer waveguide flex technology for use in optical interconnects," *J. Lightw. Technol.*, vol. 31, no. 24, pp. 3915–3926, Dec. 2013.
[29] H. Numata, M. Tokunari, and J. B. Heroux, "60-micrometer pitch polymer waveguide array attached active optical flex," in *Proc. Conf. Opt. Fiber Commun.*, Los Angeles, CA, USA, 2017, Paper W1A.5.
[30] X. Dou, X. Wang, X. Lin, D. Ding, D. Z. Pan, and R. T. Chen, "Highly flexible polymeric optical waveguide for out-of-plane optical interconnects," *Opt. Express*, vol. 18, pp. 16227–16233, 2010.
[31] T. Yagisawa *et al.*, "Structure of 25-Gb/s optical engine for QSFP enabling high-precision passive alignment of optical assembly," in *Proc. 66th Electron. Compon. Technol. Conf.*, Las Vegas, NV, USA, 2016, pp. 1099–1104.
[32] N. Bamiedakis, F. Shi, D. Chu, R. V. Penty, and I. H. White, "Flexible multimode polymer waveguides for versatile high-speed optical interconnects," in *Proc. 19th Int. Conf. Transparent Opt. Netw.*, Girona, Spain, 2017, pp. 1–4.
[33] J. Chen, N. Bamiedakis, P. Vasil'ev, R. V. Penty, and I. H. White, "Low-loss and high-bandwidth multimode polymer waveguide components using refractive index engineering," in *Proc. Conf. Lasers Electro-Opt.*, 2016, Paper SM2G.
[34] A. Hashim, N. Bamiedakis, R. V. Penty, and I. H. White, "Multimode polymer waveguide components for complex on-board optical topologies," *J. Lightw. Technol.*, vol. 31, no. 24, pp. 3962–3969, Dec. 2013.
[35] J. Chopin, V. Démery, and B. Davidovitch, "Roadmap to the morphological instabilities of a stretched twisted ribbon," *J. Elasticity*, vol. 119, pp. 137–189, 2014.
[36] J. Chopin and A. Kudrolli, "Helicoids, wrinkles, and loops in twisted ribbons," *Phys. Rev. Lett.*, vol. 111, 2013, Art. no. 174302.
[37] J. Chen, N. Bamiedakis, T. J. Edwards, C. T. Brown, R. V. Penty, and I. H. White, "Dispersion studies on multimode polymer spiral waveguides for board-level optical interconnects," in *Proc. IEEE Opt. Int. Conf.*, 2015, pp. 26–27.
[38] Z. Haas and M. A. Santoro, "A mode filtering scheme for improvement of the bandwidth distance product in multimode fiber systems," *J. Lightw. Technol.*, vol. 11, no. 7, pp. 1125–1130, Jul. 1993.
[39] J. Chen, N. Bamiedakis, P. Vasil'ev, R. V. Penty, and I. H. White, "Bandwidth enhancement in multimode polymer waveguides using waveguide layout for optical printed circuit boards," in *Proc. Conf. Opt. Fiber Commun.*, Anaheim, CA, USA, 2016, Paper W1E. 3.

Authors' biographies not available at the time of publication.